THERMODYNAMIC INVESTIGATION OF THE Ag_7GeSe_5I COMPOUND AND $Ag_{8-x}GeSe_{6-x}I_x$ SOLID SOLUTIONS BY THE EMF METHOD WITH SOLID ELECTROLYTE

N.A. Bayramova[1], I.F. Huseynova[2]*, G.B. Balakishiyeva[3], I.J. Alverdiyev[4], T.A. Aliyev[1]

[1]*Nakhchivan State University, Nakhchivan, Azerbaijan*
[2]*Institute of Chemistry, Baku, Azerbaijan*
[3]*Baku Engineering University, Baku, Azerbaijan*
[4]*Ganja State University, Ganja, Azerbaijan*
**e-mail: mehdiyeva.ilahe2@gmail.com*

Received 14.08.2025
Accepted 24.10.2025

Abstract: *Compounds of the argyrodite family and phases based on them are of considerable interest as environmentally friendly multifunctional materials exhibiting thermoelectric, photovoltaic, and optical properties, as well as high ionic conductivity. In this work, the thermodynamic properties of the Ag_7GeSe_5I compound and the solid solutions $Ag_{8-x}GeSe_{6-x}I_x$ were studied for the first time using the electromotive force (EMF) method with a solid Ag^+-conducting electrolyte Ag_4RbI_5. Based on EMF measurements of the concentration cells of the*

$$(-)Ag(s) \mid Ag_4RbI_5(s) \mid (Ag\text{–}in\ alloy)\ (+)$$

type in the 300–390 K temperature range, linear equations describing the temperature dependences of the EMF were obtained. Using these equations, the relative partial thermodynamic functions of silver in the alloys were calculated. Based on the solid-phase equilibria diagram of the Ag_2Se–AgI–$GeSe_2$ system and several boundary systems, a fragment of the phase diagram of the quaternary Ag–Ge–Se–I system was constructed. Using this diagram, the equations of the potential-forming reactions responsible for the above-mentioned partial molar functions were derived, and the standard thermodynamic functions of formation and the standard entropies of the compound Ag_7GeSe_5I and the solid solutions $Ag_{8-x}GeSe_{6-x}I_x$ (x=0.2, 0.4, 0.6, and 0.8) were calculated.

Keywords: *argyrodites, silver germanium selenoiodide, phase diagram, thermodynamic functions, superionic conductor Ag_4RbI_5*

DOI: 10.65382/2221-8688-2026-4-540-552

1. Introduction

Copper- and silver-based chalcogenides, classified as environmentally friendly materials, exhibit a wide range of functional properties, which underlie their extensive use in energy-related applications, including photovoltaics, thermoelectric devices, and batteries [1–9], as well as in medical technologies [10–12], etc.

Among the compounds mentioned, argyrodites with the general formula $A^{m+}_{(12-n)/m}B^{n+}X^{2-}_{6-x}Y^{-}_{x}$ (A^{m+} -Cu^+, Ag^+, Li^+, Zn^{2+}, Cd^{2+}, Hg^{2+}; B^{n+} - Ga^{3+}, Si^{4+}, Ge^{4+}, Sn^{4+}, P^{5+}, As^{5+}; X^{2-} - S^{2-}, Se^{2-}, Te^{2-}; Y^- -Cl^-, Br^-, I^-) occupy an important place [13–20]. Numerous studies, initiated as early as the 1960s, have demonstrated that, in addition to the aforementioned functional properties [15–18, 21–26], these compounds also exhibit superionic conductivity, enabling their use as ion-selective electrodes, solid electrolytes, and related applications [27–33]. Modifications of their composition and structure can enhance these functional properties. In particular, according to [15, 18, 28], copper- and silver-based argyrodites possess low lattice thermal conductivity and high ionic conductivity. Independent tuning of these two parameters opens up new opportunities for the development of highly efficient thermoelectric materials.

Information about the phase equilibria and thermodynamic characteristics of the related systems is necessary for the search and development of optimal technological conditions for the synthesis of new multi-component

materials with desired compositions and properties [15–17, 34–36]. As is known, a phase diagram represents the thermodynamically equilibrium state of a physicochemical system and allows for the determination of the nature of compounds formed, their thermal stability, regions of primary crystallization and homogeneity, polymorphic transitions, and so forth [15].

Systems based on ternary copper and silver argyrodites have been investigated in a number of studies, their phase diagrams have been constructed, solid solutions of various substitution types have been identified, and their crystallization processes and thermodynamic properties have been examined. [15–17, 37–46]. However, systems based on halide-containing argyrodites remain largely unexplored.

Considering the above, in our previous works [47–49], we investigated the phase equilibria in the Ag_2Se-AgI-$GeSe_2$ quasi-ternary system. A solid-phase equilibria diagram, a liquidus surface projection and several polythermal sections of the phase diagram were presented. The formation of continuous solid solutions with a cubic structure along the Ag_8GeSe_6-Ag_7GeSe_5I section was demonstrated [47].

The present work is devoted to the thermodynamic investigation of the compound Ag_7GeSe_5I and the solid solutions $Ag_{8-x}GeSe_{6-x}I_x$ by means of electromotive force (EMF) measurements using the solid electrolyte Ag_4RbI_5.

The EMF method, being one of the precise equilibrium methods in chemical thermodynamics, allows the combined investigation of phase equilibria and thermodynamic properties of metallic and semiconductor systems [50, 51]. The value of thermodynamic data obtained by the EMF method lies in the fact that, in addition to internal consistency within a given phase, they are also consistent with the phase diagram. Various modifications of this method have been successfully employed in complex studies of multicomponent chalcogenide systems [15–17, 52–59].

The presence of superionic conductors with purely Ag^+ cationic conductivity opens broad opportunities for thermodynamic investigations of complex silver-containing chalcogenides using the EMF method with a solid electrolyte. A number of studies have reported the results of such investigations for complex silver chalcogenides [15, 60–69], including compounds of the argyrodite family and phases based on them [15, 38, 44, 46, 63–66].

2. Experimental part

For the thermodynamic measurements, concentration cells of the following type were constructed:

$$(-)Ag(s) \mid Ag_4RbI_5(s) \mid (Ag\text{–in alloy})\ (+) \qquad (1)$$

The superionic conductor Ag_4RbI_5 melts at 505 K via a peritectic reaction. Below its melting temperature, Ag_4RbI_5 exhibits high and nearly pure Ag^+ ionic conductivity down to room temperature, which allows its use as a solid electrolyte in thermodynamic studies of silver-based phases over a wide temperature range [50, 69].

The Ag_4RbI_5 compound was synthesized from RbI (Alfa Aesar, 99.8%) and AgI (Alfa Aesar, 99.999%) using the following method [50, 51]: first, stoichiometric amounts of the iodides, calculated to yield 20 g of the solid electrolyte, were heated in a vacuum-sealed (~10^{-2} Pa) quartz ampoule up to 600 K. The resulting melt was then cooled to 400 K and annealed at this temperature for 200 h, ensuring complete homogenization of Ag_4RbI_5. Cylindrical ingots (~7 mm in diameter) obtained in this manner were cut into discs 4–5 mm thick and polished on a rotating polishing wheel. These prepared discs were used as the solid electrolyte in concentration cells of the type (1).

In thermodynamic studies of phases in multicomponent heterogeneous systems using the EMF method, it is crucial to have reliable data on phase equilibria within the relevant system over the temperature range of the EMF

measurements. Such data are essential both for the correct and rational planning of the experiments and for selecting the compositions of electrode alloys, as well as for processing EMF measurement data and performing accurate thermodynamic calculations based on them [50, 51].

The solid-phase equilibria diagram of the Ag_2Se-AgI-$GeSe_2$ system at room temperature is presented in Fig 1. The following phase notations are used in the diagram: α′ – the phase based on RT-Ag_2Se; δ – the solid solutions $Ag_{8-x}GeSe_{6-x}I_x$, RT-$GeSe_2$, and RT-AgI – the low-temperature modifications of the corresponding compounds.

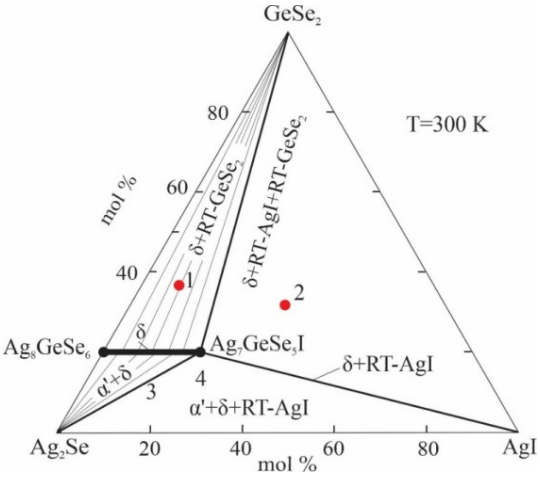

Fig. 1. Diagram of solid-phase equilibria of the Ag_2Se-$GeSe_2$-AgI system at 300 K

Considering that elemental silver is used as the reference electrode in cells of type (1), for thermodynamic studies of $Ag_{8-x}GeSe_{6-x}I_x$ solid solutions, it is advisable to use alloys from the two-phase region $Ag_{8-x}GeSe_{6-x}I_x$+$GeSe_2$ as right-hand electrodes. For the stoichiometric compound Ag_7GeSe_5I, alloys from the three-phase region Ag_7GeSe_5I+AgI+$GeSe_2$ are recommended [50, 51].

The compounds $GeSe_2$, Ag_8GeSe_6 and Ag_7GeSe_5I were synthesized for subsequent preparation of electrode alloys by co-melting mixtures of high-purity elements (Ag rod, 99.997%; Ge ingot, 99.999%; Se granules, 99.999%; I_2 powder, 99.999%) taken in stoichiometric proportions in sealed quartz ampoules under vacuum (10^{-2} Pa), as described in [47–49]. Considering the high saturated vapor pressures of iodine (T_b = 457 K) and selenium (T_b = 958 K [70]) at the melting temperatures, the syntheses were performed in a two-zone inclined furnace.

The phase purity of all synthesized starting compounds was verified by X-ray diffraction analysis (XRD) and differential thermal analysis (DTA), and the results were in agreement with the data [47–49].

Intermediate alloys from two- and three-phase regions were then obtained by melting the starting compounds in various ratios in sealed quartz ampoules. These alloys were subjected to stepwise thermal annealing at 800 K for 500 h and at 400 K for 100 h, followed by cooling in a switched-off furnace.

The phase compositions of the obtained alloys were confirmed by XRD. Fig. 2, as an example, presents powder diffractograms for two alloys with nominal compositions of 40 mol% Ag_7GeSe_5I+40 mol% Ag_8GeSe_6+ 20 mol% $GeSe_2$ (sample 1) and 60 mol % Ag_7GeSe_5I+20 mol % $GeSe_2$+20 mol % AgI (sample 2). As seen, sample 1 is two-phase, its diffraction pattern consisting of reflections from the δ-phase (solid solutions in the Ag_8GeSe_6 - Ag_7GeSe_5I system) and RT-$GeSe_2$. In contrast, the diffractogram of sample 2 exhibits peaks corresponding to RT-$GeSe_2$, RT-AgI, and Ag_7GeSe_5I, indicating its three-phase nature.

The annealed alloys were ground into fine powders and pressed into discs 7 mm in diameter and 3-4 mm thick under a pressure of ~0.1 GPa.

For EMF measurements, an electrochemical cell of the design described in [56] was assembled, evacuated, filled with argon to a pressure of ~40 kPa, and placed in a specially fabricated tubular resistance furnace, where it was thermostatted at ~360 K for three days. The cell temperature was monitored using chromel–

alumel thermocouples and a mercury thermometer with an accuracy of ±0.5 °C.

A high-impedance digital voltmeter, Keithley 2100 6½ digit, with an input resistance of 10^9 Ω was used for the EMF measurements.

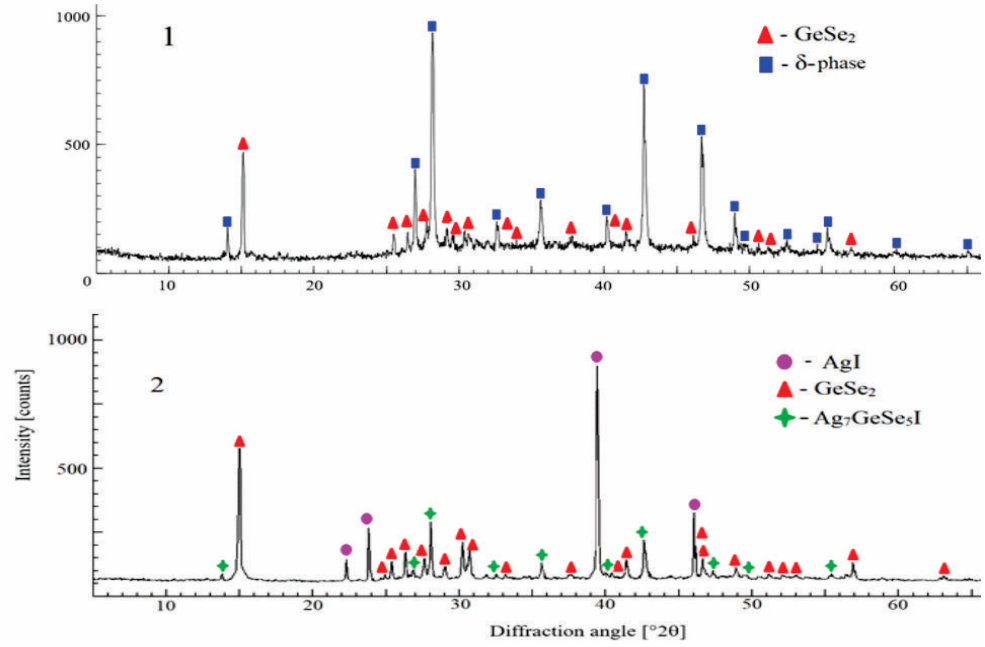

Fig. 2. Powder diffraction patterns of samples 1 and 2, shown in Fig. 1

Measurements were carried out in the temperature range of 300–390 K, within which the phase compositions of the electrode alloys are constant according to the phase diagram. EMF values were recorded every 3 hours after the set temperature was established. EMF values were considered to be at equilibrium if repeated measurements at a given temperature differed by no more than 0.5 mV, regardless of the direction of the temperature change. To monitor reproducibility, each sample was measured 2–4 times during the experiment at two constant temperatures. To eliminate the occurrence of thermoelectric EMF, the contacts of the current leads with the copper wires were maintained at the same temperature.

The reproducibility of the results obtained, as well as the constancy of the mass and phase composition of the electrodes during the experiment, confirms the reversibility of the constructed concentration cells.

3. Results and Discussion

Analysis of the EMF measurements of cells of type (1) showed that, in the studied temperature range, the EMF isotherms are monotonic functions of composition, confirming the formation of a continuous series of solid solutions (δ-phase) along the Ag_8GeSe_6-Ag_7GeSe_5I section. Furthermore, the temperature dependence for each electrode alloy is linear (Fig. 3). Accordingly, the EMF data were processed using the least-squares method under the assumption of a linear temperature dependence, yielding equations of the type (2)

$$E = a + bT \pm t\left[(S_E^2/n) + S_b^2 \cdot (T - \overline{T})^2\right]^{1/2} \quad (2)$$

recommended in contemporary thermodynamic literature [50, 51]. In equation (2), n - is the number of E and T data pairs; S_E and S_b– are the variances of individual EMF measurements and the slope coefficient b, respectively; $\overline{T}$- is the mean absolute temperature; and t- is the Student's t-statistic. At a 95 % confidence level and with n≥20 experimental points, the Student's value t≤2.

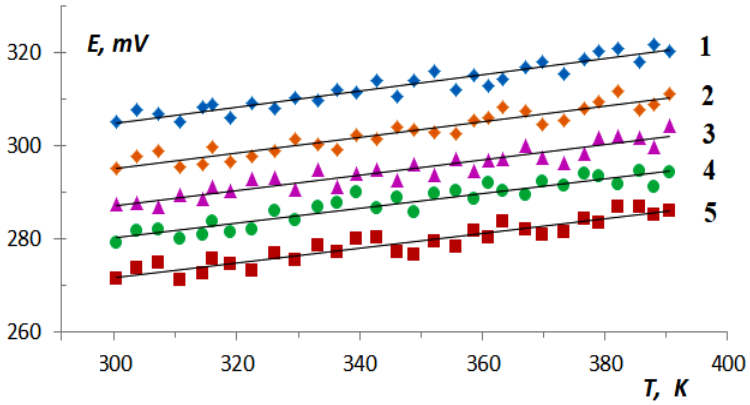

Fig. 3. Temperature dependences of the EMF for alloys from the Ag_7GeSe_5I+AgI+$GeSe_2$ region. Numbers 1–5 indicate the phase regions in Tables 1 and 2.

The resulting equations of type (2) are presented in Table 1.

Table 1. Temperature dependences of EMF for concentration cells of type (1) for Ag_8GeSe_6-Ag_7GeSe_5I alloys in the temperature range 300–390 K

№	Phase area	$E, mV = a + bT \pm 2 \cdot S_E(T)$
1	Ag_7GeSe_5I	$253.34 + 0.1721\ T \pm 2\left[\frac{2.1}{30} + 9.5 \cdot 10^{-5}(T - 346.7)^2\right]^{1/2}$
2	$Ag_{7,2}GeSe_{5,2}I_{0,8}$	$245.50 + 0.1659\ T \pm 2\left[\frac{2.3}{30} + 1.0 \cdot 10^{-4}(T - 346.7)^2\right]^{1/2}$
3	$Ag_{7,4}GeSe_{5,4}I_{0,6}$	$238.64 + 0.1620\ T \pm 2\left[\frac{2.2}{30} + 9.9 \cdot 10^{-5}(T - 346.7)^2\right]^{1/2}$
4	$Ag_{7,6}GeSe_{5,6}I_{0,4}$	$238.05 + 0.1605\ T \pm 2\left[\frac{2.0}{30} + 1.1 \cdot 10^{-4}(T - 345.2)^2\right]^{1/2}$
5	$Ag_{7,8}GeSe_{5,8}I_{0,2}$	$224.40 + 0.1574\ T \pm 2\left[\frac{2.3}{30} + 1.1 \cdot 10^{-4}(T - 345.2)^2\right]^{1/2}$

From the resulting equations (Table 1), using the known relationships [50]

$$\Delta\overline{G}_{Ag} = -zFE \qquad (3)$$

$$\Delta\overline{H}_{Ag} = -z\left[E - T\left(\frac{\partial E}{\partial T}\right)_P\right] = -zFa \qquad (4)$$

$$\Delta\overline{S}_{Ag} = zF\left(\frac{\partial E}{\partial T}\right)_P = zFb \qquad (5)$$

the relative partial thermodynamic functions of silver in the alloys were calculated (Table 2, Fig.4).

Table 2. Relative partial thermodynamic functions of silver in the Ag_8GeSe_6-Ag_7GeSe_5I alloys at 300 K.

Phase area	$-\overline{\Delta G}_{Ag}$	$-\overline{\Delta H}_{Ag}$	$\overline{\Delta S}_{Ag}$
	kJ·mol^{-1}		J·mol^{-1}·K^{-1}
Ag_7GeSe_5I + Ag_8GeSe_6	29.40±0.05	24.44±0.33	16.61±0.94
$Ag_{7,2}GeSe_{5,2}I_{0,8}$	28.46±0.05	23.69±0.34	16.00±0.98

$Ag_{7,4}GeSe_{5,4}I_{0,6}$	27.69±0.05	23.03±0.33	15.63±0.96
$Ag_{7,6}GeSe_{5,6}I_{0,4}$	27.01±0.06	22.39±0.34	15.48±0.99
$Ag_{7,8}GeSe_{5,8}I_{0,2}$	26.18±0.06	21.65±0.35	15.19±1.01
HT-Ag_8GeSe_6 [71]	25.45±0.04	21.05±0.21	14.76±0.55
RT-Ag_8GeSe_6 [71]	25.58±0.02	22.93±0.38	8.89±1.23

According to Fig. 4, the isotherms at 300 K of all three partial molar quantities of silver are continuous functions of composition and vary monotonically between the corresponding values for the high-temperature modifications of the initial ternary compounds.

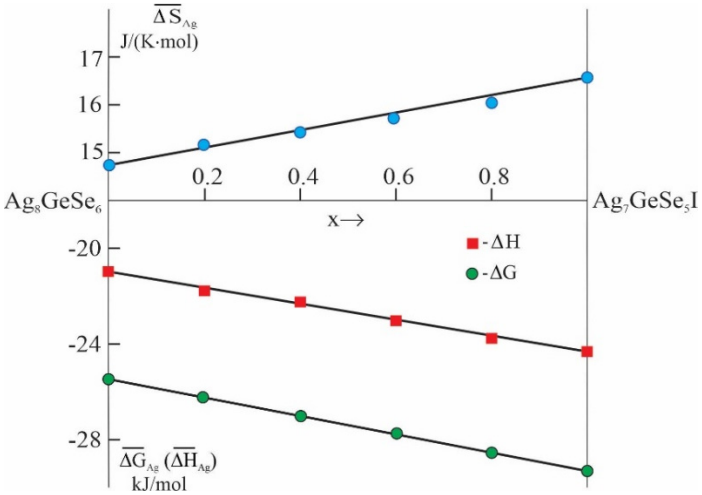

Fig. 4. Dependence of partial thermodynamic functions on the composition of alloys Ag_8GeSe_6-Ag_7GeSe_5I alloys at 300 K.

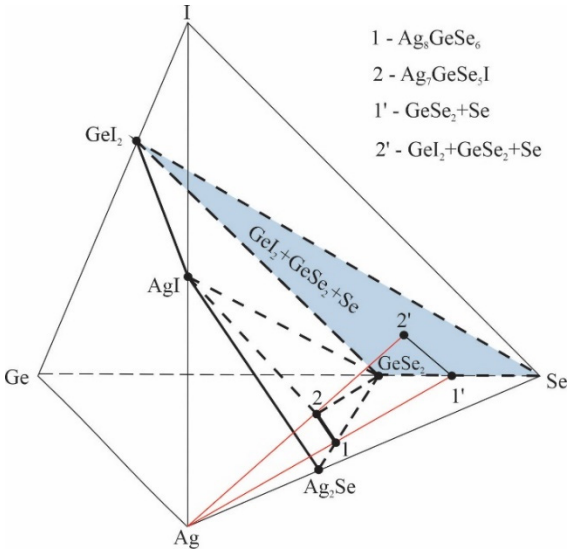

Fig. 5. Fragment of the solid-phase equilibria diagram of the Ag–Ge–Se–I system

To determine the potential-forming reactions responsible for the indicated partial molar quantities and to calculate the integral thermodynamic functions of the investigated phases of various compositions, we constructed a fragment of the solid-phase equilibria diagram of the Ag–Ge–Se–I system (Fig. 5) using Fig. 1 and literature data for the boundary systems [15, 71]. As seen in the figure, the radial line (red lines) originating from the Ag corner of the compositional tetrahedron and passing through the stoichiometric composition Ag_8GeSe_6 (point 1) reaches the Ge–Se side system in the two-phase region $GeSe_2$ + Se (point 1′). A similar radial line passing through the composition Ag_7GeSe_5I (point 2) crosses the four-phase region δ+GeI_2+$GeSe_2$+Se and reaches (point 2′) the three-phase region GeI_2-$GeSe_2$-Se (shaded

area) of the ternary Ge–Se–I system. Clearly, all radial lines passing through the Ag_8GeSe_6-Ag_7GeSe_5I section (line 1–2) reach the indicated three-phase region along the line 1′–2′. This shows that the partial molar quantities of silver in Ag_7GeSe_5I are thermodynamic functions of the following virtual potential-forming reaction (all substances in the solid state).

$$7Ag + 0.5GeI_2 + 0.5GeSe_2 + 4Se = Ag_7GeSe_5I \quad (6)$$

Then, the standard Gibbs free energy of formation and the standard enthalpy of formation of the Ag_7GeSe_5I compound can be calculated using the following relationship

$$\Delta_f Z^0(Ag_7GeSe_5I) = 7\Delta\overline{Z}_{Ag} + 0.5[\Delta_f Z^0(GeI_2) + 5\Delta_f Z^0(GeSe_2)] \quad (7)$$

where Z≡G, H, and the standard entropy is

$$S^0(Ag_7GeSe_5I) = 7[\Delta\overline{S}_{Ag} + S^0(Ag)] + 0.5[S^0(GeSe_2) + S^0(GeI_2)] + S^0(Se) \quad (8)$$

Accordingly, the overall potential-forming reaction for the solid solutions $Ag_{8-x}GeSe_{6-x}I$ can be written as

$$(8-x)\,Ag + 0.5xGeI_2 + 0.5(1-x)\,GeSe_2 + 4Se = Ag_{8-x}GeSe_{6-x}I \quad (9)$$

and the equations for calculating the standard thermodynamic functions of formation and the standard entropy, respectively, are given by

$$\Delta_f Z^0(Ag_{8-x}GeSe_{6-x}I) = (8-x)\Delta\overline{Z}_{Ag} + 0.5[x\,\Delta_f Z^0(GeI_2) + (1-x)\Delta_f Z^0(GeSe_2)] \quad (10)$$

$$S^0(Ag_{8-x}GeSe_{6-x}I) = (8-x)[\Delta\overline{S}_{Ag} + S^0(Ag)] + 0.5[xS^0(GeI_2) + (1-x)S^0(GeSe_2)] + 4S^0(Se) \quad (11)$$

In the calculations, the recommended values of the standard entropies of silver, germanium, and selenium from modern reference literature were used ($S^o(Ag) = 42.55 \pm 0.13$ J·mol^{-1}·K^{-1}; $S^o(Ge) = 31.09 \pm 0.13$ J·mol^{-1}·K^{-1}; $S^o(Se) = 42.13 \pm 0.21$ J·mol^{-1}·K^{-1}) [72], as well as the standard integral thermodynamic functions of the compounds $GeSe_2$ and GeI_2 (Table 3). The standard enthalpy of formation and entropy of $GeSe_2$ were taken from [72, 73], while the corresponding values for GeI_2 were taken from [74]. The standard Gibbs free energies of formation of both compounds were calculated based on these data using the Gibbs–Helmholtz equation.

The results of the calculations according to equations (7), (8), (10), and (11) are presented in Table 3. Data from [63] for the two crystalline modifications of Ag_8GeSe_6 are also provided for comparison.

Table 3. Standard integral thermodynamic functions of phases in the Ag_8GeSe_6 - Ag_7GeSe_5I system and the compounds GeI_2 and $GeSe_2$

Phase	$-\Delta_f G^0$(298 K)	$-\Delta_f H^0$ (298 K)	$\Delta_f S^0$ (298 K)	S^0(298 K)
	кJ/mol		J·(mol·K)	
$GeSe_2$	101.3±2.9	102.3±2.6 [73]	-	112.6±3.4 [72]
GeI_2	91.0±6.5	88.1±6.1[74]	-	157.0±0.2 [74]
Ag_7GeSe_5I	302.0±5.1	266.3±6.9	120.0±7.5	717±10
$Ag_{7,2}GeSe_{5,2}I_{0,8}$	302.2±4.7	267.3±6.5	116.4±7.5	721±11
$Ag_{7,4}GeSe_{5,4}I_{0,6}$	303.1±4.4	268.4±6.0	116.4±7.5	725±11
$Ag_{7,6}GeSe_{5,6}I_{0,4}$	304.3±4.0	269.5±5.9	116.7±7.6	731±12

$Ag_{7,8}GeSe_{5,8}I_{0,2}$	304.7±3.8	269.9±5.6	116.7±7.6	736±12
HT-Ag_8GeSe_6 [63]	305.1±3.4	270.7±4.2	115.4±9.0	741±14
RT-Ag_8GeSe_6 [63]	306.0±3.1	285.7±5.7	68.1±13	694±19

At first glance, the data in Table 3 may give the impression that the thermodynamic functions of formation of the phases in the Ag_8GeSe_6–Ag_7GeSe_5I system change little with composition. However, this is not the case. This apparent invariance arises because the presented data refer to formula units, and as the phase composition changes from Ag_7GeSe_5I to Ag_8GeSe_6, the number of atoms per formula unit changes from 14 to 15. If the data were expressed per an equal number of atoms, the numerical values would differ significantly.

Conclusion

Thus, for the first time, a comprehensive set of mutually consistent thermodynamic data has been obtained for the compound Ag_7GeSe_5I and the solid solutions $Ag_{8-x}GeSe_{6-x}I_x$. The investigations were carried out by EMF measurements of concentration cells relative to a silver electrode, using a solid Ag^+-conducting electrolyte. Linear equations representing the temperature dependence of EMF were established for each analyzed phase based on these results. The relative partial Gibbs free energy, enthalpy, and entropy of silver in the alloys were derived from these equations. A schematic equilibria diagram of the quaternary Ag–Ge–Se–I system was constructed to ascertain the virtual potential-forming reactions associated with these partial molar quantities, utilizing the solid-phase equilibria diagram of the Ag_2Se–AgI–$GeSe_2$ system and relevant literature data for boundary systems. The standard integral thermodynamic functions of formation and standard entropies for the Ag_7GeSe_5I compound and the solid solutions $Ag_{8-x}GeSe_{6-x}I_x$ with compositions x = 0.2, 0.4, 0.6, and 0.8 were computed based on this diagram. The thermodynamically described argyrodite phases are significantly intriguing as eco-friendly thermoelectric materials and combined ionic-electronic conductors.

References

1. Applications of Chalcogenides: S, Se, and Te. Ahluwalia G. K. (ed.). Cham. Springer, 2016. 461 p. DOI: 10.1007/978-3- 319-41190-3
2. Alonso-Vante N. Chalcogenide materials for energy conversion. In: Nanostructure Science and Technology. Springer International Publishing. 2018. 226 p. DOI: 10.1007/978-3-319-89612-0
3. Khan M.M. Chalcogenide-Based Nanomaterials as Photocatalysts, Amsterdam: Elsevier. 2021.
4. Salehabadi A., Enhessari M., Ahmad M.I., Ismail N., Gupta B.D. Metal Chalcogenide Biosensors: Fundamentals and Applications. 1st ed., Woodhead Publishing. 2023. 214 p.
5. Devika R.S., Vengatesh P., Shyju T.S. Review on ternary chalcogenides: Potential photoabsorbers. *Materials Today: Proccedings*, 2023, DOI: 10.1016/j.matpr.2023.04.113
6. Liu W., Yang L., Chen Z., Zou J. Promising and Eco-Friendly Cu_2X-Based Thermoelectric Materials: Progress and Application. *Advanced Materials*, 2020, **Vol. 32(8),** 1905703. DOI: 10.1002/adma.201905703
7. Tee S.Y., Ponsford D., Lay C.L., Wang X., Wang X., Chi D., Neo J., Wu T., Thitsartarn W., Chee J., Yeo C., Guan G., Lee T., Han M. Thermoelectric Silver-Based Chalcogenides. *Advanced Science*, 2022, **Vol. 9(36),** 2204624. DOI: 10.1002/advs.202204624
8. Deng Y., Wei M., Lei Y., Lu J., Peng P., Zhang Y., Zheng Z. Advances in silver-based chalcogenide flexible thermoelectric. *CrystEngComm,* 2025, **Vol. 27(8)**, p. 1055–1077. DOI:10.1039/D4CE00915K
9. Ram M., Sapna R., Rondiya S.R., Hareesh K.A review on copper-based chalcogenide materials for supercapacitor application:

Exploring through experimental evidence and machine learning. *Journal of Materials Chemistry A*, 2025, **Vol. 13,** p. 40448–40489. DOI: 10.1039/D5TA04689K

10. Nieves L.M., Mossburg K., Hsu J.C., Andrew D., Maidment A., Cormode P., Ram M., Sapna R., Rondiya S.R., Hareesh K. Silver chalcogenide nanoparticles: a review of their biomedical applications. *Nanoscale*, 2021, **Vol. 13,** p. 19306-19323. DOI: 10.1039/D0NR03872E
11. Mao Q., Ma J., Chen M., Lin S., Razzaq N., Cu J. Recent advances in heavily doped plasmonic copper chalcogenides: from synthesis to biological application. *Chemical Synthesis,* 2023, **Vol. 3**, p. 26-41. DOI: 10.20517/cs.2022.41.
12. Ivanchenko M., Jing H. Smart Design of Noble Metal–Copper Chalcogenide Dual Plasmonic Heteronanoarchitectures for Emerging Applications: Progress and Prospects. *Chemistry of Materials*, 2023, **Vol. 35(12),** p. 4598–4620. DOI: 10.1021/acs.chemmater.3c00346.
13. Hahn H., Schulze H., Sechser L. Über einige ternäre Chalkogenide vom Argyrodit-Typ. *Naturwissenschaften,* 1965, **Vol. 52(11)**, 451. in German. DOI: 10.1007/BF00627053
14. Gorochov O. Les composes Ag_8MX_6 (M = Si, Ge, Sn et X = S, Se, Te). *Bulletin de la Société chimique de France,* 1968, **Vol. 101(6)**, p. 2263-2275 in French.
15. Babanly M.B., Yusibov Y.A., Imamaliyeva S.Z., Babanly D.M., Alverdiyev I.J. Phase diagrams in the development of the argyrodite family compounds and solid solutions based on them. *Journal of phase equilibria and diffusion*, 2024, **Vol. 45**, p. 228-255. DOI: 10.1007/s11669-024-01088-w.
16. Babanly M.B., Mashadieva L.F., Imamaliyeva S.Z., Babanly D.M., Taghiyev D.B., Yusibov Y.A. Complex copper-based chalcogenides: a review of phase equilibria and thermodynamic properties. *Condensed Matter and Interphases*, 2024, **Vol. 26(4),** p. 579-619. DOI: 10.17308/kcmf.2024.26/12367.
17. Babanly M.B., Mashadiyeva L.F., Imamaliyeva S.Z., Tagiev D.B., Babanly D.M., Yusibov Yu.A. Thermodynamic properties of complex copper chalcogenides. *Chemical Problems*, 2024, **Vol. 22(3),** p. 243-280. DOI: 10.32737/2221-8688-2024-3-243-280
18. Lin S., Li W., Pei Y. Thermally insulative thermoelectric argyrodites. *Materials Today,* 2021, **Vol. 48**, p. 198-213. DOI: 10.1016/j.mattod.2021.01.007.
19. Laqibi M., Cros B., Peytavin S., Ribes M. New silver superionic conductors Ag_7XY_5Z (X = Si, Ge, Sn; Y = S, Se; Z = Cl, Br, I) – Synthesis and electrical studies. *Solid State Ion,* 1987, **Vol. 23(1-2),** p. 21-26. DOI: 10.1016/0167-2738(87)90077-4
20. Nagel A., Range K.J., Die Kristallstruktur von Ag_7GeS_5I. *Zeitschrift für Naturforschung B,* 1979, **Vol. 34**, p. 360-362. DOI: 10.1515/znb-1979-0246
21. Parashchuk T., Cherniushok O., Wiendlocha B., Tobola J., Cardoso-Gil R., Jeffrey Snyder G., Grin Y. High Thermoelectric Performance in Low-Cost $Cu_8SiS_xSe_{6-x}$ Argyrodite. *Advanced Functional Materials,* 2025, **Vol 35(34),** 2502163. DOI: 10.1002/adfm.202502163
22. Haruna A.Y., Luo Y., Li W., Ma Z., Yang L., Zhang Z., Jiang Q., Li X., Liu H., Yang J. High thermoelectric performance in multiscale Ag_8SnSe_6 included n-type bismuth telluride for cooling application. *Materials Today Energy*, 2023, **Vol. 35,** 101332. DOI: 10.1016/j.mtener.2023.101332.
23. Yang C., Xia Y., Xu L., Luo Y., Li X., Han Z., Cui J. Enhancement of thermoelectric performance of argyrodite Ag_8GeSe_6 via isoelectronic substitution of Sn for Ge. *Chemical Engineering Journal*, 2021, **Vol. 426,** 131752. DOI: 10.1016/j.cej.2021.131752.
24. Munsif M., Neffati R., Shah M., Khan S., Ashraf M.W., Murtaza G. First principles study of the structural, mechanical, and optical properties of argyrodite-structured Ag6PS5X (X= Br, I) compounds. *Solid State Communications,* 2023, **Vol. 371**, 115245. DOI: 10.1016/j.ssc.2023.115245
25. Semkiv I., Ilchuk H., Pawlowski M., Kusnezh V. Ag_8SnSe_6 argyrodite synthesis and optical

properties. *Opto-Electronics Review*, 2017, **Vol. 25(1),** p. 37-40
26. Yang M., Shao G., Wu B., Jiang J., Liu S., Li H. Irregularly Shaped Bimetallic Chalcogenide Ag_8SnS_6 Nanoparticles as lectrocatalysts for Hydrogen Evolution. *ACS Applied Nano Materials,* 2021, **Vol. 4(7),** p. 6745–6751. DOI: 10.1021/acsanm.1c00769
27. Ayoola O.M., Buldum A., Farhad S., Ojo S.A. A Review on the Molecular Modeling of Argyrodite Electrolytes for All-Solid-State Lithium Batteries, *Energies,* 2022, **Vol. 15(19),** 7288. DOI: 10.3390/en15197288
28. Wu X., Liang L., Du B., Liu Y., Zhang Z., Shi Y., Tang S., Hou G., Zhou H., He P. High-Conductivity Argyrodite Electrolyte with Self-Passivating Stability for Single-Electrolyte All-Solid-State Lithium Batteries. *Angewandte Chemie International Edition*, 2026, **Vol. 65(4),** e23225. DOI: 10.1002/anie.202523225
29. Sardarly R.M., Ashirov G.M., Mashadiyeva L.F., Aliyeva N.A., Salmanov F.T., Agayeva R.Sh., Mamedov R.A., Babanly M.B. Ionic conductivity of the Ag_8GeSe_6 compound. *Modern Physics Letters B*, 2022, **Vol. 36(32-33)**, 2250171. DOI: 10.1142/S0217984922501718
30. Sardarly R.M, Babanly M.B., Aliyeva N.A., Mashadiyeva L.F., Mamadov R., Ashirov G.M., Saddinova A., Damirova S. Obtaining and Measuring Impedance Characteristics of the Ag_8SiSe_6 Compound. *East European Journal of Physics*, 2025, **Vol. 1,** p. 233-239. DOI: 10.26565/2312-4334-2025-1-24
31. Ghata A., Eckert P.L., Böger T., Garg P., Zeier W.G. Influence of Cu^+ Substitution on the Structural, Ionic, and Thermal Transport Properties of $Ag_{8-x}Cu_xGeS_6$ Argyrodites. *Chemistry of Materials,* 2025, **Vol. 37(17),** p. 6900–6911. DOI: 10.1021/acs.chemmater.5c01679.
32. Albert S., Pillet S., Lecomte C., Pradela A., Ribes M. Disorder in Ag_7GeSe_5I, a superionic conductor: temperature-dependent anharmonic structural study. *Acta Crystallographica*, 2008, **Vol. 64**, p. 1–11. DOI: 10.1107/S0108768107059642
33. Studenyak I.P., Pogodin A.I., Luchynets M.M., Studenyak V.I., Kokhan O.P., Kus P. Impedance studies and electrical conductivity of $(Cu_{1x}Ag_x)_7GeSe_5I$ mixed crystals. *Journal of Alloys and Compounds*, 2020, **Vol. 817,** 152792. DOI: 10.1016/j.jallcom.2019.152792.
34. Cantor B. Exploring Multicomponent Phase Space to Discover New Materials. *Journal of phase equilibria and diffusion,* 2024, **Vol. 45**, p. 188–218. DOI:10.1007/s11669-024-01131-w
35. Saka H. Introduction to phase diagrams in materials science and engineering. World Scientific Publishing Co. 2020. 188 p.
36. Imamaliyeva S.Z., Huseynova I.F., Daraselia D., Japaridze D., Shengelaya A., Babanly M.B. Phase Relations in the Tl_2Te-$TlBiTe_2$-$TlGdTe_2$ Compositions Region of the Tl-Bi-Gd-Te System and Magnetic Properties of the $TlBi_{1-x}Gd_xTe_2$ solid Solutions. *Journal of phase equilibria and diffusion,* 2024, **Vol. 45**, p. 459-468. DOI: 10.1007/s11669-024-01096-w
37. Amiraslanova A.J., Mammadova A.T., Imamaliyeva S.Z., Alverdiyev I.J., Yusibov Yu.A., Babanly M.B. The $6Ag_2Se+Ag_8GeTe_6 \leftrightarrow 6Ag_2Te+Ag_8GeSe_6$ reciprocal system. *Russian Journal of Inorganic Chemistry*, 2023, **Vol. 68(8),** p. 1054-1064. DOI: 10.31857/S0044457X2360024X.
38. Aslanli S.R., Alverdiyev I.J., Imamaliyeva S.Z., Jafarov Y.I., Yusibov Y.A., Babanly M.B. Phase Relations in the Ag_2S-Ag_8SiS_6-Ag_8SnS_6 System and Thermodynamic Properties of Polymorphic Transitions of Argyrodite Phases. *International Journal of Thermophysics,* 2025, **Vol. 46**, p. 26-45. DOI: 10.1007/s10765-025-03501-z
39. Poladova A.N., Huseynova I.F., Alverdiyev I.J., Gasymov V.A., Mashadiyeva L.F., Babanly M.B. Phase equilibria and high-entropy alloys in the Cu_8GeSe_6-Ag_8GeS_6 system. *Russian Journal of Inorganic Chemistry*, 2025, **Vol. 70(11)**, p. 1778-1784. DOI: 10.1134/S0036023625602132
40. Ismailova E.N., Mashadieva L.F., Bakhtiyarly I.B., Gasymov V.A., Huseynova I.F., Dzhafarov Ya.I. Experimental study of phase equilibria in the Cu_2SnSe_3-Cu_3SbSe_4-Se ternary system. *Condensed Matter and Interphases*, 2025,

Vol. 27(4), p. 606-614. DOI: 10.17308/kcmf.2025.27/13298

41. Ashirov G.M., Babanly K.N., Mashadiyeva L.F., Yusibov Y.A., Babanly M.B. Phase equilibra in the Ag_2Se–Ag_8GeSe_6–Ag_8SiSe_6 system and characterization of the $Ag_8Si_{1-x}Ge_xSe_6$ solid solution. *Chemical Problems*, 2023, **No 3,** p. 229-241. DOI: 10.32737/2221-8688-2023-3-229-241
42. Bayramova U.R., Babanly K.N., Ahmadov E.I., Mashadiyeva L.F., Babanly M.B. Phase equilibria in the Cu_2S-Cu_8SiS_6-Cu_8GeS_6 system and thermodynamic functions of phase transitions of the $Cu_8Si_{(1-X)}Ge_xS_6$ argyrodite phases. *Journal of Phase Equilibria and Diffusion*, 2023, **Vol. 44**, p. 509–519. DOI: 10.1007/s11669-023-01054-y.
43. Bayramova U.R., Poladova A.N., Mashadiyeva L.F., Babanly M.B. Calorimetric determination of phase transitions of Ag_8BX_6 (B=Ge, Sn; X=S, Se) compounds. *Condensed Matter and Interphases*, 2022, **Vol. 4(2),** p. 187–195. DOI: 10.17308/kcmf.2022.24/9258
44. Alverdiyev I.J., Imamaliyeva S.Z., Akhmedov E.I., Yusibov Yu.A., Babanly M.B. Thermodynamic properties of some ternary compounds of the argyrodite family. *Azerbaijan Chemical Journal*, 2023, **No 4**, 21–30. DOI: 10.32737/0005-2531-2023-4-21-30.
45. Bayramova U.R., Babanly D.M., Mashadiyeva L.F., Akhmedov E.I., Babanly M.B. Calorimetric study of phase transition of the Cu_8GeSe_6 and comparison with other argyrodite family compounds. *Chemical Problems*, 2023, **No 4,** p. 396-403. DOI: 10.32737/2221-8688-2023-4-396-403.
46. Amiraslanova A.J., Mammadova A.T., Imamaliyeva S.Z., Alverdiyev I.J., Yusibov Yu.A., Babanly M.B. Thermodynamic investigation of Ag_8GeTe_6 and $Ag_8GeTe_{6-x}Se_x$ solid solutions by the EMF method with a solid Ag^+ conducting electrolyte. *Russian Journal of Electrochemistry*, 2023, **Vol. 59(12),** p. 834–842. DOI: 10.31857/S0424857023120034.
47. Huseynova I.F., Bayramova N.A., Imamaliyeva S.Z., Aliyeva A.Sh., Yusibov Yu.A., Babanly M.B. Phase equilibria in the Ag_8GeSe_6-Ag_7GeSe_5I-$GeSe_2$ system, *Russian Journal of Inorganic Chemistry.* 2025, **Vol. 70(11),** p. 1793–1802. DOI: 10.1134/S0036023625602533
48. Bayramova N.A., Huseynova I.F., Melikova E.T., Imamaliyeva S.Z. Phase relations in the AgI-Ag_7GeSe_5I-$GeSe_2$ system. *Journal of Chemical and Material Sciences*, 2025, **Vol. 2(3),** p. 36-42. DOI: 10.30546/209501.201.2025.2.003.012
49. Bayramova N.A., Hüseynova İ.F., Əliyev T.A. AgI-$GeSe_2$ sistemində faza tarazlıqları. *Naxçıvan Dövlət Universitetinin elmi əsərlər jurnalı,* 2025**, № 3,** s.1-7. DOI: 10.64400/ea25-3-22
50. Morachevskii A.G., Voronin G.F., Geiderikh V.A. Electrochemical Methods of Investigation in the Thermodynamics of Metallic Systems. Akademkniga Publishing Center, Moscow, 2003, 334 p.‡in Russian].
51. Babanly M.B., Yusibov Yu.A. Electrochemical methods in the thermodynamics of inorganic systems (in Russian). Baku. Elm. 2011. 306 p.
52. Imamaliyeva S.Z., Mehdiyeva I.F., Gasymov V.A., Babanly D.M., Taghiyev D.B., Babanly M.B. Solid-Phase Equilibria and Thermodynamic Properties of Phases in the Tm–Te System. *Russian Journal of Physical Chemistry A,* 2021, **Vol. 95(4),** p. 926-932. DOI: 10.1134/S0036024421050149
53. Mashadiyeva L.F., Babanly D.M., Hasanova Z.T., Yusibov Yu.A., Babanly M.B. Phase Relations in the Cu-As-S System and Thermodynamic Properties of Copper-arsenic Sulfides. *Journal of Phase Equilibria and Diffusion*, 2024, **Vol. 45(3),** p. 567–582. DOI: 10.1007/s11669-024-01115-w
54. Mammadov F.M., Babanly D.M., Imamaliyeva S.Z., Huseynova I.F., Moroz M.V., Abbasova V.A., Bakhtiyarly I.B., Babanly M.B. Solid-phase relations in the FeSe-Ga_2Se_3-Se system and thermodynamic investigation of the $FeGa_2Se_4$ compound and $(FeSe)_{1-x}(Ga_2Se_3)_x$ solid solutions. *Chemical Thermodynamics and Thermal Analysis*, 2025, 100207. DOI: 10.1016/j.ctta.2025.100207
55. Nabiyev E.R., Orujlu E.N., Babanly D.M., Imamaliyeva S.Z., Yusibov Y.A., Babanly M.B. Standard Thermodynamic Functions

of Sb_2Te_3-Rich Germanium Antimony Tellurides: EMF Measurement. *International Journal of Thermophysics,* 2025, **Vol. 46(10)**, 158. DOI: 10.1007/s10765-025-03631-4

56. Hasanova G.S., Aghazade A.I.,Babanly D.M., Imamaliyeva S.Z., Yusibov Y.A., Babanly M.B. Experimental study of the phase relations and thermodynamic properties of Bi-Se system. *Journal of Thermal Analysis and Calorimetry*, 2022, **Vol. 147,** p. 6403–6414. DOI: 10.1007/s10973-021-10975-0
57. Hasanova G.S., Aghazade A.I., Imamaliyeva S.Z., Yusibov Y.A., Babanly M.B, Refinement of the Phase Diagram of the Bi-Te System and the Thermodynamic Properties of Lower Bismuth Tellurides. *JOM*, 2021, **Vol. 73(5),** p. 1511-1521. DOI: 10.1007/s11837-021-04621-1
58. Aliev Z.S., Musayeva S.S. Imamaliyeva S.Z., Babanlı M.B. Thermodynamic study of antimony chalcoiodides by EMF method with an ionic liquid. *Journal of Thermal Analysis and Calorimetry*, 2018, **Vol. 133(2),** p. 1115-1120. DOI: 10.1007/s10973-017-6812-4
59. Okajima K., Sakao H. On the New Method of Determining the Activities in Molten Alloys-The Touch Instant Electromotive Force Method. *Transactions of the Japan Institute of Metals*, 1968, **Vol. 9(1),** p. 47-53. DOI: 10.2320/matertrans1960.9.47
60. Moroz M.V., Tesfaye F., Demchenko P., Prokhorenko M., Prokhorenko S., Reshetnyak O. Non-activation synthesis and thermodynamic properties of ternary compounds of the Ag–Te–Br system. *Thermochimica Acta*, 2021, **Vol. 698**, 178862(1–7 pages). DOI: 10.1016/j.tca.2021.178862
61. Moroz M.V., Tesfaye F., Demchenko P., Prokhorenko M., Yarema N., Lindberg D., Reshetnyak O., Hupa L. The equilibrium phase formation and thermodynamic properties of functional tellurides in the Ag–Fe–Ge–Te system. *Energies,* 2021, **Vol. 14(5),** 1314(1–15 pages). DOI: 10.3390/en14051314
62. Moroz M.V., Tesfaye F., Demchenko P., Prokhorenko M., Kogut Yu., Pereviznyk O., Prokhorenko S., Reshetnyak O. Solid-state electrochemical synthesis and thermodynamic properties of selected compounds in the Ag–Fe–Pb–Se system. *Solid State Sciences*, 2020, **Vol. 107**, 106344(1–9 pages). DOI: 10.1016/j.solidstatesciences.2020.106344
63. Alverdiyev I.Dzh., Bagheri S.M., Imamaliyeva S.Z., Yusibov Y.A., Babanly M.B. Thermodynamic study of Ag_8GeSe_6 by EMF with an Ag_4RbI_5 solid electrolyte. *Russian Journal of Electrochemistry*, 2017, **Vol. 53(5),** p. 511-554. DOI: 10.1134/S1023193517050032
64. Aslanli S.R., Alverdiyev I.J., Imamaliyeva S.Z., Jafarov Y.I., Yusibov Y.A., Babanly M.B. Phase Relations in the Ag_2S-Ag_8SiS_6-Ag_8SnS_6 System and Thermodynamic Properties of Polymorphic Transitions of Argyrodite Phases. *International Journal of Thermophysics*, 2025, **Vol. 46**, p. 26. DOI: 10.1007/s10765-025-03501-z
65. Aslanly S.R., Imamaliyeva S.Z., Ashirov G.M., Alverdiyev I.J., Yusibov Yu.A., Babanly M.B. Study of thermodynamic properties of HT-Ag_8SiSe_6 and $Ag_8Si_{1-x}Sn_xSe_6$ solid solutions by the EMF method with a solid electrolyte. *Russian Journal of Electrochemistry,* 2025, **Vol. 61(12),** p. 858-867. DOI: 10.1134/S1023193525120058.
66. Alverdiev I.D., Imamalieva S.Z., Babanly D.M., Yusibov Yu.A., Tagiev D.B., Babanly M.B. Thermodynamic Study of Siver—Tin Selenides by the EMF Method with Ag_4RbI_5 Solid Electrolyte. *Russian Journal of Electrochemistry*, 2019, **Vol. 55(5),** p. 467–474. DOI: 10.1134/S1023193519050021
67. Kristavchuk A.V., Zabolotskaya A.V., Voronin M.V., Chareev D.A., Osadchii E.G. Temperature dependence of tellurium fugacity for the kotulskite (PdTe)–merenskyite ($PdTe_2$) equilibrium determined by the method of a solid-state galvanic cell. *Physics and Chemistry of Minerals,* 2021, **Vol. 48**, p. 16. DOI: 10.1007/s00269-021-01141-x
68. Osadchii E.G., Voronin M.V. Thermodynamic Properties of $RuTe_2$ Evaluated by EMF Measurements on a Solid State Electrochemical Cell. *Inorganic Materials,* 2024, **Vol. 60(3),**

p. 832–837. DOI: 10.1134/S0020168524701061
69. Ivanov-Shchits A.K., Murin I.V. Solid State Ionics. **Vol. 1.** St. Petersburg State University Press. St. Petersburg. 2000. 616 p.
70. Emsley J. *The Elements*. second edition. London. Clarendon press. 1993. 256 p
71. Massalski T.B. *Binary Alloy Phase Diagrams*. 2nd Edition, ASM International. Materials Park. OH. 1990. 3589 p.
72. *Database of thermal constants of substances*. Electronic version. Ed.: Iorish V.S. and Jungman V.S. 2006. http://www.chem.msu.su/cgi-bin/tkv.
73. O'Hare P.A.G. Susman S., Volin K.J. The energy difference between the crystalline and vitreous forms of germanium diselenide as determined by combustion calorimetry in fluorine. The Ge-Se bond energy. *Journal of Non-Crystalline Solids*, 1987, **Vol. 89(1–2),** p. 24-30. DOİ:10.1016/0022-3093(87)90304-3
74. Zelenina L.N., Titov V.A., Chusova T.P., Stenin Yu.G., Titov A.A. On the thermodynamic properties of germanium-iodide compounds. *The Journal of Chemical Thermodynamics*, 2023, **Vol. 35(10)**, p. 1601-1612. DOİ: 10.1016/S0021-9614(03)00123-X